Jagannath University Journal of Science
Volume 08, Number II, June 2022, pp. 7–14
https://jnu.ac.bd/journal/portal/archives/science.jsp
ISSN 2224-1698

Shallow Folded Potential for α+^{24}Mg Elastic Scattering

Research Article

Shuva Saha, Proma Modal, Dipika Rani Sarker and M. Nure Alam Abdullah*

Department of Physics, Jagannath University, Dhaka-1100, Bangladesh

Received: 03 April 2022
Accepted: 15 May 2022

Abstract: The experimental angular distributions of α+^{24}Mg elastic scattering are analyzed using the shallow folded potential in the framework of the optical model (OM). The present folded potential is constructed using both alpha-alpha (α–α) and alpha-nucleon (α–N) interactions. The best-fits to the experimental data yield the number of nucleons making α-like cluster $4A_\alpha = 20.0$ and the number of unclustered nucleons $A_N = 4.0$ in a time-averaged picture. The volume integral per nucleon pair for the real part of the potential has been found to vary between $J_R/(4A) = -188.9$ MeV.fm^3 and $J_R/(4A) = -166.9$ MeV.fm^3 in the energy range E_α = 28.0-81.0 MeV. The root-mean-square radius has been deduced and found to be 3.033 fm.

Keywords: *Folded potential • Optical model • Alpha cluster • Renormalization*

1. Introduction

The knowledge of nucleus-nucleus interaction is important as it provides the basic understanding of the structure of matter as well as the universe at the deepest level. Various methods have been used to describe the phenomena for a quite long time including those with a sharp cut-off in the nuclear potential and those containing a diffuseness parameter in the nuclear potential. To explain the scattering due to nuclear forces *i.e.* to fit the angular distributions of the emitted particle, the nuclear potential is to be taken into account. There are a number of potentials to explain various nuclear properties. Out of them, the optical model (OM) potential enjoys success in explaining nuclear scattering for a quite long time since it can explain the loss of flux from the incident channel to the outgoing channels.

The unusual enhancement of cross section at large angles, initially observed for ^{16}O and ^{32}S by Correlli *et al.* (1959), is a prominent feature of the α-induced elastic scattering data from the light nuclei for incident energies up to about 50 MeV. Since then it has been found for a number of different targets up to ^{48}Ca (Gruhn *et al.*, 1966 and Wall *et al.*, 1975). This enhancement of cross section is termed as anomaly in large angle scattering (ALAS). The ALAS effect is prominent for targets of mass $A = 4n$ ($n = 0, 1, 2, \ldots$). As the energy of the incident α-particle increases, the ALAS effect dies down and gives rainbow scattering with fall in cross sections beyond a certain angle of scattering. The ALAS effect makes the α-particle elastic scattering a challenging one. Over the last six decades, different types of α-nucleus potentials have been tried to fit the experimental angular distributions of α elastic scattering. The Woods-Saxon (WS) potential, although can successfully explain the nucleon-nucleus scattering, fails to describe the elastic scattering of α-particles (Kemper *et al.*, 1972). The squared WS (SWS) potential (Michel *et al.*, 1986, Michel *et al.*, 1995) and non-monotonic (NM) potential (Tariq *et al.*, 1999, Abdullah *et al.*, 2002, Abdullah *et al.*, 2005) have been found successful in explaining the α elastic scattering on different targets including the ALAS. Folded potential is also a good candidate and often used to construct the α-nucleus potentials.

* Corresponding author: M. Nure Alam Abdullah
E-mail: abdullah@phy.jnu.ac.bd

Microscopic double-folded (DF) potential of nucleon-nucleon (*N*-*N*) interaction (Kobos *et al.*, 1984, Atzrott *et al.*, 1996, Khoa, 2001) and semi-microscopic single-folded (SF) potential of either α-N or α-α interaction (Li and Yang 1993, Yang and Li 1993, M. El-Azab Farid 1990, Farid *et al.* 2001, Singh *et al*. 1975, Neu *et al*. 1989) have been found satisfactory in accounting for the elastic scattering of α-particles from various nuclear targets. However, a renormalization factor $N_r = 0.84 - 1.39$ (Kobos *et al.* 1984, Li and Yang 1993, Yang and Li 1993) is required for the folded potentials (both DF and SF) to account for the experimental α elastic scattering data. For α+^{12}C and α+^{16}O elastic scattering, Khallaf *et al.* (1997) could manage to have $N_r = 1$ in terms of a complex folded potential using two additional parameters, β_R and β_I, which, in turn, renormalize their potential. Farid *et al.* (2001) employed SF potentials of α–α interaction to fit the experimental α+^{16}O elastic scattering data at energies between 32.2 and 146.0 MeV using an energy-dependent renormalization factor. In his work, D. T. Khoa (2001) analyzed the angular distributions of cross section for three α energies *viz*. 54.1, 80.7 and 104.0 MeV using DF potentials of realistic density dependent modified 3-parameter Yukawa (DDM3Y) interaction. Here again, the renormalization factor had been found to be $N_r = 0.97 - 1.14$ and the experimental data were limited to about 100^0 scattering angles. Avrigeanu *et al.* (2003) used a DF potential to describe the α elastic scattering data on ^{89}Y and ^{90,91}Zr without any renormalization. However, they had to use a difficult calculation that included a density dependent N-N interaction, an energy-dependent factor with an extra parameter, the exchange integral and the dispersion effect (Mahaux and Ngô 1982, Nagarajan *et al*. 1985, Mahaux *et al*. 1986) of the imaginary potential on the real potential. Ornelas *et al*. (2015) analyzed the α-particle elastic scattering on ^{106}Cd for incident energies ranging from 15.6 to 26.0 MeV in terms of DF potential using *N*-*N* interaction parameterized by DDM3Y interaction. All the folded potentials, discussed here, are deep in nature with volume integrals for the real part $J_R/(4A) \approx -300$ MeV.fm^3.

In 2003, Abdullah *et al.* (2003, 2003) suggested a single-folding model of mixed α-α and α-N configurations, the resultant SF potential from which does not require any renormalization. They were able to explain the elastic scattering of α-particles by ^{16}O, $^{40.44,48}$Ca, ^{58,60,62}Ni, ^{28}Si and ^{90}Zr targets for a wide range of incident energies using this modified SF (MSF) potential (Abdullah *et al.*, 2003, Abdullah *et al.*, 2003, Billah *et al*., 2005, Abdullah and Shil 2014, Abdullah *et al*., 2014). Hossain *et al*. (2006) satisfactorily described the experimental ^{16}O+^{12}C elastic scattering data using the MSF potential. In their works, Hassanain *et al.* (2008, 2013) successfully used the MSF potential to account for the ^{12}C+^{12}C and ^{16}O+^{16}O elastic scattering data. Like other folded potentials (both DF and SF), the MSF potentials are also deep in nature.

Tariq *et al*. (1999) satisfactorily described the α+^{24}Mg elastic scattering using the shallow NM ($J_R/(4A) = -116.1$ MeV.fm^3) and deep SWS ($J_R/(4A) = -227.4$ to -487.7 MeV.fm^3) potentials. Abdullah *et al*. (2016) analyzed the elastic scattering of α-particles from ^{24}Mg in terms of the deep MSF potential with real volume integrals from $J_R/(4A) = -329.8$ MeV.fm^3 to $J_R/(4A) = -382.5$ MeV.fm^3 derived from the single-folding model of Abdullah *et al*. (2003). The prime purpose of the present work is to analyze the experimental angular distributions of α+^{24}Mg elastic scattering at incident energies $E_\alpha = 28 - 81$ MeV in terms of shallow MSF potential with $|J_R/(4A)| < 200$ MeV.fm^3 without any renormalization.

Section 2 of this article presents the theoretical formalism of the MSF potential. The analyses of the data and derived results are presented in section 3. Discussion on results and conclusions are drawn in section 4.

2. Theory

α-clustering provides wide-ranging applications in nuclear reactions and nuclear structure. Because of the high symmetry and high binding energy of α-particles, nucleons inside the nucleus are likely to condense into particles and live long enough to affect many properties of nuclei as well as the cross sections of nuclear reactions, particularly those with particles as the projectile.

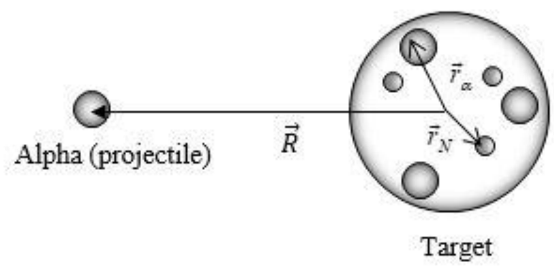

Figure 1. Single-folding model of Abdullah *et al.* (2003). The larger spheres in the target nucleus are the α-cluster and smaller spheres are the unclustered nucleons.

Following the work of Block *et al*. (1971), a system of the projectile (α-particle) and the target nucleus having A nucleons in the metastable state has been considered. The wave function Ψ of the composite system at a given time can be expanded in terms of an orthonormal set of wave function Φ_n as

$$\Psi(1, \ldots, A+4) = \sum_n A_n \Phi_n(1, \ldots\ldots, A+4). \qquad (1)$$

Here, the summation is over all coordinates $(1, \ldots, A+4)$.

The amplitude A_n, in Eq. (1), is the scalar product of the wave functions Φ_n and Ψ, i.e, $A_n = (\Phi_n, \Psi)$ and determines the amount of a particular configuration present in the composite system at a particular time. In the target-projectile system, both Φ_n and the total Hamiltonian H can be expressed in terms of the relative coordinate $\boldsymbol{R}$ of the alpha-target system and the intrinsic coordinates of nucleons in the incident α and the target nuclei marked as primes with anti-symmetrization:

$$\Phi_n = \sum_{i\beta} f_{ni\beta}(\boldsymbol{R})\psi_{ni}(1', \ldots .A')\phi_{n\beta} \times [(A+1)' \ldots \ldots (A+4)'], \quad (3)$$

and

$$H = -\frac{\hbar^2}{2M}\nabla_R{}^2 + H_o(1', \ldots, A') + H_\alpha[(A+1)', \ldots, (A+4)'] + H_{int}\,[\boldsymbol{R}, 1', \ldots, (A+4')]. \quad (4)$$

In Eq. (4), M is the reduced mass, H_{int} denotes the potential between the nucleons in the incident α-particle and the nucleons in the target nucleus. Orthonormality condition gives the following relation:

$$\left[\frac{\hbar^2}{2M}\left(\nabla_R{}^2 + k_{ni\beta}{}^2\right) + V_{nnii\beta\beta}(\boldsymbol{R}) + K_{nnii\beta\beta}(\boldsymbol{R})\right] f_{ni\beta}(\boldsymbol{R}) = \sum\left[V_{mnij\beta\mu}(\boldsymbol{R}) + K_{mnij\beta\mu}(\boldsymbol{R})\right] f_{mi\mu}(\boldsymbol{R}). \quad (5)$$

Here, the summation on the right side stands for all cases except $m = n$, $i = j$ and $\mu = \beta$.

The potential $V_{mnij\beta\mu}(\boldsymbol{R})$ is given by

$$V_{mnij\beta\mu}(\boldsymbol{R}) = \left(\psi_{ni}\varphi_{n\beta}, H_{int}\psi_{mj}\varphi_{m\mu}\right), \quad (6)$$

where, ψ_{ni} and $\varphi_{n\beta}$, respectively denote the wave functions of H_0 and H_α with eigenvalues E_{ni} and $E_{n\beta}$ satisfying

$$\hbar^2 k_{ni\beta}^2/2M = E - E_{ni} - E_{n\beta}.$$

In Eq. (5), $K_{mnij\beta\mu}(\boldsymbol{R})$ denotes the non-local potential arising from the Pauli principle. If we consider the projectile α as an isolated boson, in the first approximation, we can neglect the exchange contributions of the incident α-particle with α-like cluster as well as with single fermion-like configurations in the target nucleus. Furthermore, in the absence of sharp resonance, the energy- averaged contribution of the coupling terms leads to a complex potential (Feshbach, 1958 and 1962). In this approximation, denoting the average α-nucleus potential by $U(R)$ due to H_{int}, Eq. (5) can be written, after dropping the subscripts, by

$$\left[-\frac{\hbar^2}{2m}(\nabla^2 + k^2) + U(R)\right] f(R) = 0. \quad (7)$$

Equation (6) now assumes the form

$$U(R) = V_{nnii\beta\beta} = \left(\psi_{ni}\varphi_{n\beta}, H_{int}\psi_{ni}\varphi_{n\beta}\right). \quad (8)$$

If $(1, 2, \ldots, x)$ nucleons exist in cluster-like state and $\big((x+1), \ldots, A\big)$ nucleons in unclustered nucleonic state in the target, then denoting the center of mass coordinate of the projectile α by $\boldsymbol{R}_\alpha$ and the coordinates of the nucleons in α-like cluster and unclustered nucleons as indexed by i and j respectively, Eq. (8) can be cast in the following approximate form:

$$U(R) = \left(\psi_{ni}\varphi_{n\beta}(\boldsymbol{R}_\alpha), \left[\sum_{i=1}^{x} H_{int}(\boldsymbol{R}, |\boldsymbol{r}_i - \boldsymbol{R}_\alpha|) + \sum_{j=x+1}^{A} H_{int}\left(\boldsymbol{R}, |\boldsymbol{r}_j - \boldsymbol{R}_\alpha|\right)\right]\psi_{ni}\varphi_{n\beta}\right). \quad (9)$$

Now approximating wave function of the target nucleus by,

$$\psi_{ni}(1', \ldots, A') \approx \phi_\alpha(1', \ldots \ldots, x')\phi_N((x+1)', \ldots \ldots A'). \quad (10)$$

with ϕ_α and ϕ_N are the wave functions of the α-like and unclustered nucleonic configurations respectively and integrating over $\boldsymbol{R}_\alpha$, one can write Eq. (9) in the form

$$U(R) = \left(\phi_\alpha(1', \ldots, x')\phi_N((1+x)', \ldots, A')\left[\sum_{i=1}^{x} V_{\alpha\alpha}(|\boldsymbol{R} - \boldsymbol{r}_i|) + \sum_{j=x+1}^{A} V_{\alpha N}\left(|\boldsymbol{R} - \boldsymbol{r}_j|\right)\right]\phi_\alpha(1', \ldots, x')\phi_N((1+x)', \ldots, A')\right). \quad (11)$$

Here, $V_{\alpha\alpha}$ and $V_{\alpha N}$ are respectively the potentials of the projectile with the α-like clusters and with unclustered nucleons in the target nucleus.

If $\rho_\alpha(\boldsymbol{r}_\alpha)$ and $\rho_N(\boldsymbol{r}_N)$ are respectively the density distributions (DDs) of the α-like clusters and unclustered nucleons in the target, the MSF potential, given in Eq. (11), can be written as

$$U(R) = \int \rho_\alpha(\boldsymbol{r}_\alpha)V_{\alpha\alpha}(|\boldsymbol{R} - \boldsymbol{r}_\alpha|)d^3\boldsymbol{r}_\alpha + \int \rho_N(\boldsymbol{r}_N)V_{\alpha N}(|\boldsymbol{R} - \boldsymbol{r}_N|)d^3\boldsymbol{r}_N. \quad (12)$$

The 3-parameter Fermi (3pF) DD function (De Vries *et al.* 1987) for $\rho_\alpha(\boldsymbol{r}_\alpha)$ and $\rho_N(\boldsymbol{r}_N)$ has been used and is given by

$$\rho_i(r) = \rho_{0i}\left(1 + w\frac{r^2}{c_i^2}\right)\left[1 + \exp\left(\frac{r - c_i}{a_i}\right)\right]^{-1}, \quad (13)$$

with $i = \alpha, N$.

Assuming that the target nucleus is composed of A_α α-clusters with $4A_\alpha$ nucleons and A_N unclustered nucleons, then the normalization integral can be written (Abdullah *et al.* 2003) as

$$\int \rho_\alpha(\boldsymbol{r}_\alpha)d^3\boldsymbol{r}_\alpha + \int \rho_N(\boldsymbol{r}_N)d^3\boldsymbol{r}_N = 4A_\alpha + A_N = A_T. \quad (14)$$

If the value of the parameters in the density distributions $\rho_\alpha(\boldsymbol{r}_\alpha)$ and $\rho_N(\boldsymbol{r}_N)$ are such that the integral value A_T in Eq. (14) is different from the target mass number A, then one may define the renormalization factor N_r as

$$A_T(E) = N_r(E)A. \tag{15}$$

According to the assumptions given in (Abdullah *et al*. 2003, Abdullah *et al*. 2003) including the basic premise of Ali and Bodmer (1966), the α-α potential can be expressed as

$$V_{\alpha\alpha}(r) = V_R \exp(-\mu_R^2 r^2) - V_A \exp(-\mu_A^2 r^2), \tag{16}$$

where, V_R and V_A are respectively the depths of the repulsive and attractive parts of the α-α potential with μ_R and μ_A as their range parameters.

For the α–N potential, the following form (Ali *et al*. 1985) has been taken:

$$V_{\alpha N}(r) = -V_0 \exp(-k^2 r^2), \tag{17}$$

where, k is the range parameter.

The following phenomenological Gaussian potential is used in conjunction with the real potential:

$$W(R) = -W_0 \exp\left(-\frac{R^2}{R_W{}^2}\right) - W_S \exp\left[-\left(\frac{R-D_S}{R_S}\right)^2\right]. \tag{18}$$

The Coulomb potential $V_C(R)$ is given by

$$V_C(R) = \begin{cases} \frac{Z_1 Z_2 e^2}{2R_C}\left(3 - \frac{R^2}{R_C{}^2}\right), & R \le R_C \\ \frac{Z_1 Z_2 e^2}{R}, & R > R_{C,} \end{cases} \tag{19}$$

where, the Coulomb radius is $R_C = r_C A^{1/3}$.

3. Analysis and Results

The α+^{24}Mg elastic scattering data have been taken from Neu *et al*. (1989) which contain cross sections over a complete range of scattering angles. The experimental data have been analyzed using the optical model code SCAT2 (Bersillon, *private communication*) in conjunction with the χ^2 minimization code MINUIT (James and Roos, 1975). The parameters of the MSF potential have been obtained by minimizing χ^2 defined by

$$\chi^2 = \frac{1}{N}\sum_i \left[\frac{\sigma_{exp}(\theta_i) - \sigma_{th}(\theta_i)}{\Delta\sigma_{exp}(\theta_i)}\right]^2. \tag{19}$$

Here $\sigma_{\exp}(\theta_i)$ is the experimental cross section with $\Delta\sigma_{\exp}(\theta_i)$ as its error at the angle θ_i. $\sigma_{th}(\theta_i)$ is the calculated cross section using the MSF potential and N is the number of data points for a particular projectile energy.

To generate the shallow MSF α-^{24}Mg potentials, the experimental data have been analyzed at 6 energy points namely 28.0, 42.0, 50.0, 54.0, 67.0 and 81.0 MeV using the 3pF density distribution, given in Eq. (13). The analyses have been carried out using the complete α-α interaction including both attractive and repulsive parts, and the α-N interaction. In the analyses, the parameter values, $V_A = 122.62$ MeV and $\mu_A = 0.469$ fm^{-1} in Eq. (16) have been taken from Buck *et al*. (1977); $V_A = 47.3$ MeV and $k = 0.435$ fm^{-1} in (3.38), from Sack *et al*. (1954). The Coulomb radius parameter $r_C = 1.35$ fm together with the values of V_A, μ_A, V_0 and k have been kept fixed throughout the whole range of incident energies. The parameters w, c_α and a_α of the α-density distribution, given in Eq. (13), have been taken from De Vries *et al*. (1987). The diffuseness parameter a_N of the unclustered nucleonic density distribution has been kept same as that a_α of the α-density distribution. The value of c_N has been adjusted for the best fits to the whole range of α+^{24}Mg elastic scattering data, which has been found to be $c_N = 1.50$ fm. The values of $\rho_{0\alpha}$ and ρ_{0N} have been kept fixed for all the incident α energies and found to be 0.03538 fm^{-3} and 0.1995 fm^{-3} respectively in order to satisfy the normalization integral in Eq. (14). The values of density parameters, and the energy independent best-fit parameters along with the root mean square radius of the shallow MSF α-^{24}Mg potentials are noted in Table 1.

Table 1. Energy independent parameters of the density distributions and the deduced results. $\rho_{0\alpha}$ and ρ_{0N} are in fm^{-3}; c_α, c_N, $a_\alpha = a_N$, and R_{rms} are in fm.

$\rho_{0\alpha}$	ρ_{0N}	c_α	c_N	$a_\alpha = a_N$	w	$4A_a$	A_N	A	N_r	R_{rms}
0.03538	0.1995	3.108	1.50	0.607	–0.163	20.0	4.0	24.0	1.0	3.033

The values of geometry parameters R_W, D_S and R_S of the imaginary potential, the depth parameters V_R, W_0, and W_S, and the volume integrals J_R/(4A) and J_I/(4A) respectively, for the real and imaginary parts of the MSF α-^{24}Mg potentials at different incident energies are listed in Table 2. The range parameter, μ_1 of the repulsive part of the α-α potential has been found to be $\mu_1 = 0.61$ fm^{-1} for the best overall fits to the experimental data. The parameter, R_W of the volume imaginary potential has been kept fixed and found to be $R_W = 3.80$ fm. The real part of the MSF α-^{24}Mg potential has volume integrals ranging from $J_R/(4A) - 180.9$ MeV.fm^3 to $J_R/(4A) - 166.9$ MeV.fm^3 in the energy range $E_\alpha = 18.0 - 81.0$ MeV. This sort of volume integrals for the real part has been found typically for the shallow potential. The volume integral for the imaginary part of the potential varies between $J_I/(4A) - 72.16$ and $J_R/(4A) - 127.0$ MeV.fm^3 in the same energy range. Equation (14) gives the deduced values of the normalization integrals as $4A_\alpha = 20.0$, $A_N = 4.0$ and $A = 24.0$. According to Eq. (15), since $A_T = A$, the renormalization factor has been found as N_r =1.0.

Table 2. Energy dependent parameters along with the volume integrals and χ^2. E_α, V_R and W_0 are in MeV; R_W, D_S and R_S, in fm; and $J_R/(4A)$ and $J_I/(4A)$, in MeV.fm^3.

E_α	V_R	μ_1	W_0	R_W	W_S	R_S	D_S	$J_R/(4A)$	$J_I/(4A)$	χ^2
28	290	0.67	17.5	3.80	4.0	0.645	6.0	–180.9	–72.16	21.37
42	297		18.0		4.5			–174.8	–76.22	55.99
50	300		21.0		5.0			–172.1	–87.63	27.64
54	302		26.0		5.0			–170.4	–102.33	32.12
67	304		27.0		7.5			–168.7	–118.22	8.60
81	306		30.0		7.8			–166.9	–127.04	9.42

In Fig. 2, the calculated cross sections, using the shallow MSF potentials are compared as solid curves with the experimental α+^{24}Mg elastic scattering data shown as open circles at 6 energy points from 28.0 to 81.0 MeV. It is evident from the figure that the shallow MSF potential, without any renormalization, produces satisfactory fits to the differential α+^{24}Mg elastic scattering data in the energy range 28.0-81.0 MeV.

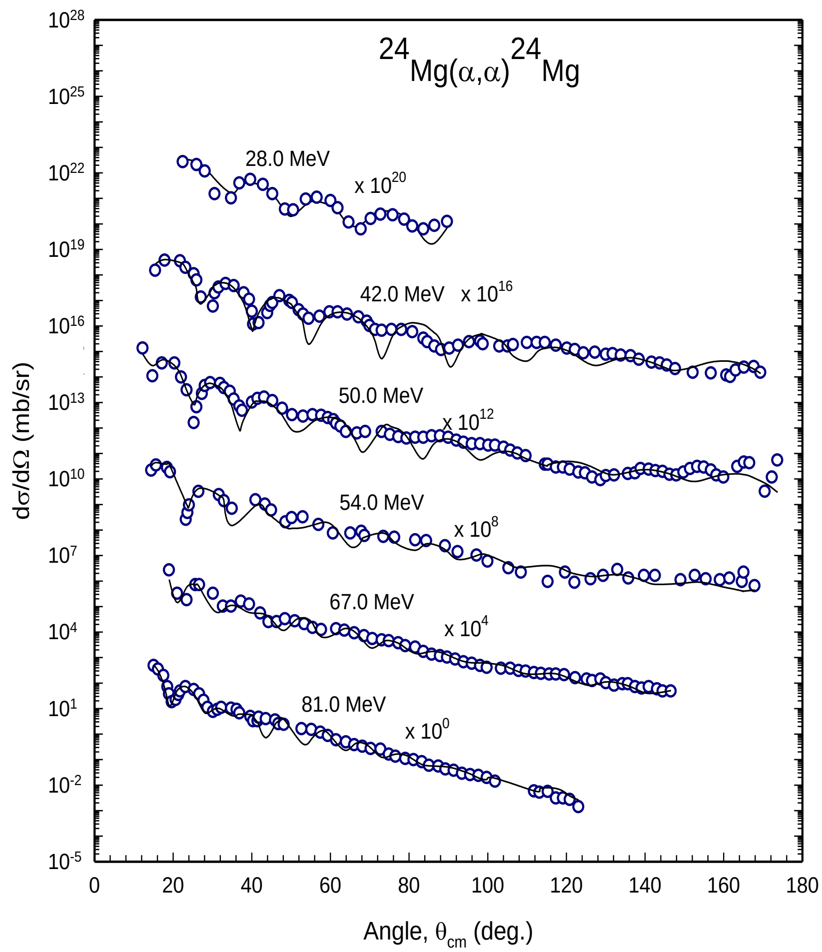

Figure 2. The predicted cross sections (solid curves) using the shallow MSF potentials with 3pF DD functions are compared with the experimental data (open circles) for the α+^{24}Mg elastic scattering at incident energies $E_\alpha = 28 - 81$ MeV. The experimental data are taken from Neu *et al*. (1989).

3.1. Energy Dependence of Volume Integrals

The energy dependence of the volume integrals $J_R/(4A)$ and $J_I/(4A)$, respectively, for the real and imaginary parts of the MSF α-^{24}Mg are also studied in the present work. We have employed the following analytic relations for the energy dependence of $J_R/(4A)$ and $J_I/(4A)$ respectively:

$$J_R = J_{R0} + aE_\alpha + bE_\alpha^2, \tag{19}$$

$$J_I = J_{I0} + aE_\alpha + bE_\alpha^2. \tag{20}$$

Here J_R stands for $J_R/(4A)$ and J_I stands for $J_I/(4A)$. In Eq. (19), for the real volume integral, the values of the coefficients are: $J_{R0} = 198.4$, $a = -0.754$ and $b = 0.0045$. For the imaginary volume integral given in Eq. (20), the coefficient values are: $J_{I0} = 42.34$, $a = -0.858$ and $b = 0.0028$. Figures 3 and 4 respectively display the variation of $J_R/(4A)$ and $J_I/(4A)$ with incident α energy. Here the solid circles are the values of $J_R/(4A)$ and $J_I/(4A)$ obtained from the analysis, and solid curves represent the analytical fits using the relation given in Eqs. (19) and (20) respectively.

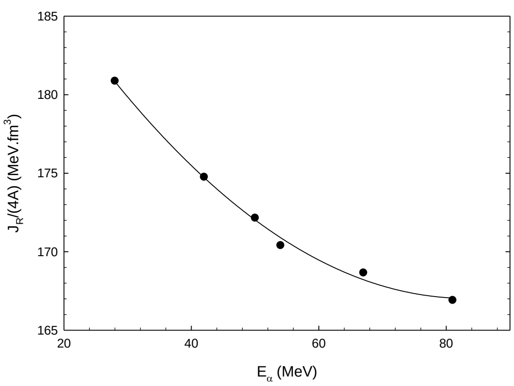

Figure 3. Energy dependence of J_R/(4A) for the MSF α-^{24}Mg potentials obtained from the analysis of the present study. The solid circles are the values of J_R/(4A) obtained from the analysis and the solid curve is the analytical fit to J_R/(4A) using Eq. (19).

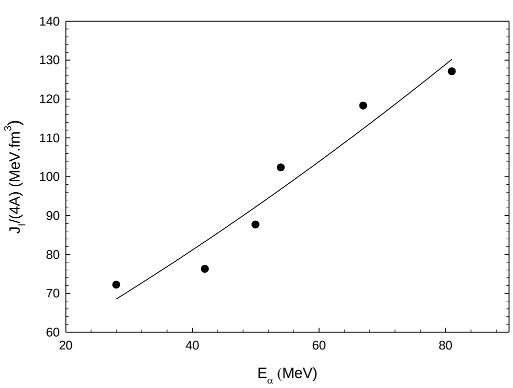

Figure 4. Energy dependence of J_I/(4A) for the MSF α-^{24}Mg potentials. The solid circles are the values of J_I/(4A) obtained from the analysis and the solid curve is the analytical fit to J_I/(4A) using Eq. (20).

3.2. Energy Dependence of W_0 and W_S

The energy dependence of the depth parameters, W_0 and W_S of the volume imaginary and surface imaginary potentials respectively for the α-^{24}Mg interaction are sought through the following relations:

$$W_0 = W_{00} + aE_\alpha + bE_\alpha^2, \tag{21}$$

$$W_S = W_{S0} + aE_\alpha + bE_\alpha^2. \tag{22}$$

Here $W_{00} = 9.593$, $a = 0.2468$ and $b = 0.0001$ are found for Eq. (21), and $W_{S0} = 3.129$, $a = 0.006$, $b = 0.007$, for Eq. (22). The analytical fits to the energy dependence of W_0 is shown in Fig. 5 and that of W_S is displayed in Fig. 6. In these figures, the solid circles are the values of W_0 and W_S obtained from the analysis of the experimental data and the solid curves are the analytical fits to W_0 and W_S using Eqs. (21) and (22) respectively.

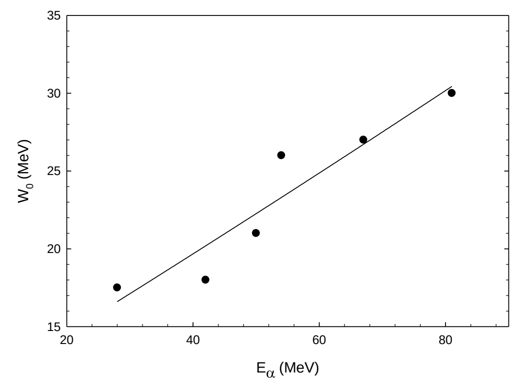

Figure 5. Energy dependence of the volume imaginary depth, W_0 of the MSF α-^{24}Mg potential.

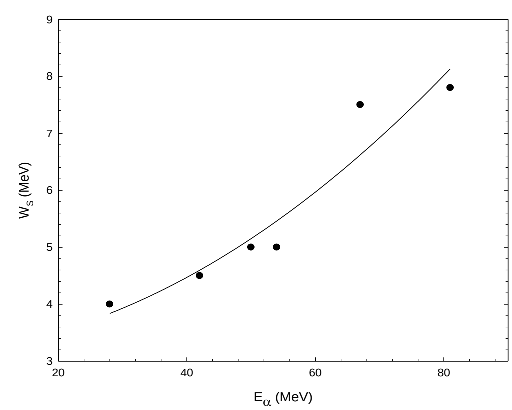

Figure 6. Energy dependence of the surface imaginary depth, W_S of the MSF α-^{24}Mg potential.

4. Discussion and Conclusions

The aim of the present work is to seek for the *shallow* folded potential for the α+^{24}Mg elastic scattering. In this regard, the experimental angular distributions of α+^{24}Mg elastic scattering are analyzed at six energy points between 28.0 and 81.0 MeV. The study has been carried out with the consideration of the MSF potential resulting from the single-folding model of Abdullah *et al.* (2003). In this model, the target nucleus ^{24}Mg is considered to be composed primarily of α-like clusters and the rest of the time in unclustered nucleonic configuration.

The fits to the data are shown in Fig. 2 in which an excellent agreement is observed between the experimental angular distributions and the theoretical predictions obtained from the MSF potential. The volume integral per nucleon pair $J_R/(4A)$ for the real part of the potential has been found to vary between $J_R/(4A) = -180.9$ MeV.fm^3 and $J_R/(4A) = -166.9$ MeV.fm^3 in the energy range E_α = 28.0-81.0 MeV. The integral values are slightly higher than those for a typical shallow nucleus-nucleus potential [$J_R/(4A)$~100 MeV.fm^3] (Tariq *et al.* 1999). However, the volume integral for a deep nucleus-nucleus potential is about −300 MeV.fm^3. (Abdullah *et al.*, 2005) Therefore, it can be fairly said that the potentials found in this work belong to the family of shallow nucleus-nucleus potential.

The real part of the shallow MSF potential for the α+^{24}Mg system, used in this work, comprises of three components, namely, (i) the attractive part of the α-α potential, (ii) the α-α repulsive part and (iii) the attractive α-N potential. The derived MSF potentials, employing the parameters V_A and μ_A for the attractive part of α-α interaction and those V_0 and k for the α-N potential are taken from the literature and kept unchanged for all the incident energies. The resulting potential is, therefore, semi-microscopic in nature. The 3pF DD functions, used in the present study, generate five α-like clusters with $4A_\alpha$ = 20.0 nucleons in them, and A_N = 4.0 unclustered nucleons in the target ^{24}Mg in a time-averaged picture. This means that all the 24 nucleons in the target ^{24}Mg participate in generating the MSF α-^{24}Mg potential which does not require any renormalization over the entire range of α energies.

The present analysis of the α+^{24}Mg elastic scattering data using the shallow MSF potentials suggests that the unclustered nucleonic density distribution has much smaller radius than the radius of the α-like clusters (Table 1). This is in agreement with the works of Abdullah *et al*. (2003, 2003, 2014), Billah *et al*. (2005) in which they showed that the formation of α-particle is energetically favoured in the surface region of a nucleus. However, this confinement of the unclustered nucleons to a smaller radius contradicts the works of Hartmann *et al.* (2001, 2002). The root mean square (rms) radius of the shallow MSF α-^{24}Mg potential has been deduced and found to be $R_{rms} = 3.80$ fm. The obtained value of the rms radius agrees well with the compilation of De Vries *et al.* (1987).

As a consequence of the present study, it seems that an acceptable form of the α-nucleus potential emerges out from the view of the single-folding model of Abdullah *et al*. (2003) which can solve the long standing renormalization problem which persists with other deep α-nucleus potentials (Kobos *et al*. 1984, Michel *et al*. 1986, Khoa 2001, Yang and Li 1993, Farid *et al*. 2001, Avrigeanu *et al*. 2003, Ornelas *et al*. 2015). The success of the single-folding model of Abdullah *et al*. (2003) is again attributed in the present work to confirm the use of elastic scattering as a significant probe to study the α-clustering in nuclei.

References

Abdullah MNA, Mahbub MS, Das SK, Tariq ASB, Uddin MA, Basak AK, Sen Gupta HM, Malik FB. (2002). Investigation of α-nucleus interaction in the ^{27}Al(α,α)^{27}Al scattering and ^{27}Al(α,d)^{29}Si reaction. *Eur. Phys. J. A*, 15: 477-486.

Abdullah MNA, Hossain S, Sarker MS, Das SK, Tariq AS, Uddin MA, Basak AK, Ali S, Sen Gupta HM, Malik FB. (2003). Cluster structure of ^{16}O. *Eur. Phys. J. A*, 18(1): 65-73.

Abdullah MNA, Sarker MS, Hossain S, Das SK, Tariq AS, Uddin MA, Mondal AS, Basak AK, Ali S, Gupta HS, Malik FB. (2003). Cluster structure of ^{40,44,48}Ca. *Phys. Lett. B*, 571(1-2): 45-49.

Abdullah MNA, Idris AB, Tariq ASB, Islam MS, Das SK, Uddin MA, Mondal AS, Basak AK, Reichstein I, Sen Gupta HM, Malik FB. (2005). Potentials for the α-^{40,44,48}Ca elastic scattering. *Nucl. Phys. A*, 760: 40-58.

Abdullah MNA, Shil RR. (2014). Semi-microscopic folded potentials for the α+^{28}Si elastic scattering. *Bang. J. Phys.*, 16: 29-37.

Abdullah MNA, Hossain S, Hossain SM Al, Hossain T, Sarker DR. (2014) Modified single-folded potentials for the α+^{90}Zr elastic scattering. *Bang. J. Phys*., 16: 67-75.

Abdullah MNA, Sudipta SB, Sarker DR. (2016). Folded potential description of the α+^{24}Mg elastic scattering. *Bang. J. Phys*., 19: 107-114.

Ali S, Bodmer AR. (1966). Phenomenological α-α potentials. *Nucl. Phys*., 80 (1): 99-112.

Ali S, Ahmad AA, Ferdous NA. 1985. Survey of the alpha-nucleon interaction. *Rev. Mod. Phys*.,57(4): 923.

Atzrott U, Mohr P, Abele H, Hillenmayer C, Staudt G. (1996). Uniform α-nucleus potential in a wide range of masses and energies. *Phys. Rev. C*, 53: 1336-1347.

Avrigeanu M, Von Oertzen W, Plompen A, Avrigeanu V. (2003). Optical Model Potentials for Alpha-Particles Scattering around the Coulomb Barrier on A-100 Nuclei. *Nucl. Phys. A*, 723: 104-126.

Bersillon O. The code SCAT2, NEA 0829, *private communication.* Billah MM, Abdullah MNA, Das SK, Uddin MA, Basak AK, Reichstein I, Gupta HS, Malik FB. (2005). Alpha-Ni optical model potentials. *Nucl. Phys. A*, 762(1-2): 50-81.

Block B, Clark JW, High MD, Malmin R, Malik FB. (1971). Fission and the Ion-Ion Interaction. *Ann. Phys. (New York)*, 62: 464-491.

Buck B, Friedrich H, Wheatley C. (1977). Local potential models for the scattering of complex nuclei. *Nucl. Phys. A*, 275(1): 246-268.

Correlli JC, Bleuler E, Tendam DJ. (1959). Scattering of 18-Mev Alpha Particles by C^{12}, O^{16}, and S^{32}. *Phys. Rev.*, 116: 1184-1193.

De Vries H, De Jager CW, De Vries C. (1987). Nuclear charge-density-distribution parameters from elastic electron scattering. *At. Data Nucl. Data Tables*, 36(3): 495-536.

Farid M El-Azab. (1990). Four-alpha cluster folding model of^{16}O-ions. *J. Phys. G*, 16: 461-467.

Farid M El-Azab, Mahmoud ZMM, Hassan GS. (2001). α-clustering folding model. *Phys. Rev. C*, 64: 014310.

Feshbach H. (1958). Unified theory of nuclear reactions. *Ann. Phys.* (*N.Y.*), 5(4): 357-390.

Feshbach H. (1962). Unified theory of nuclear reactions II. *Ann. Phys.* (*N.Y.*), 19(2): 287-313.

Gruhn CR, Wall NS. (1966). Large-angle elastic scattering of alpha particles by ^{39}K, ^{40}Ca, ^{42}Ca, ^{44}Ca and ^{50}Ti. *Nucl. Phys.*, 81: 161-179.

Hartmann FJ, Schmidt R, Ketzer B, von Egidy T, Wycech S, Smolańczuk R, Czosnyka T, Jastrzębski J, Kisieliński M, Lubiński P, Napiorkowski P. (2001). Nucleon density in the nuclear periphery determined with antiprotonic x rays: Calcium isotopes. *Phys. Rev. C*, 65(1): 014306.

Hartmann T, Enders J, Mohr P, Vogt K, Volz S, Zilges A. (2002). Dipole and electric quadrupole excitations in ^{40,48}Ca. *Phys. Rev. C*, 65(3): 034301.

Hassanain MA, Ibraheem AA, Farid M El-Azab. (2008). Double folding cluster potential for C^{12}+C^{12} elastic scattering. *Phys. Rev. C*, 77(3): 034601.

Hassanain MA, Ibraheem Awad A, Sebiey SMMA, Mokhtar SR, Zaki MA, Mahmoud ZMM, Behairy KO, Farid, M. El-Azab. (2013). Investigation of ^{16}O+^{16}O elastic scattering using the α-cluster folding model. *Phys. Rev. C*, 87(6): 064606.

Hossain S, Abdullah MNA, Hasan KM, Asaduzzaman M, Akanda MA, Das SK, Tariq AS, Uddin MA, Basak AK, Ali S, Malik FB. (2006). Shallow folding potential for ^{16}O+^{12}C elastic scattering. *Phys. Lett. B*, 636(5): 248-252

James F, Roos M. (1975). MINUIT: a system for function minimization and analysis of the parameter errors and corrections. *Comput. Phys. Commun*., 10:343-367.

Kemper KW, Obst AW, White RL. (1972). Elastic Scattering of Alpha Particles from ^{27}A1 in the Energy Range 21-28 MeV. *Phys. Rev. C*, 6: 2090-2095.

Khallaf SAE, Amry AMA, Mokhtar SR. (1997). Elastic scattering analysis of α and ^{3}He particles on ^{12}C and ^{16}O using a complex folded potential. *Phys. Rev. C*, 56(4): 2093-2103.

Khoa DT. 2001. α-nucleus optical potential in the double-folding model. *Phys. Rev. C*, 63: 034007.

Kobos AM, Brown BA, Lindsay R, Satchler GR. (1984). Folding-model analysis of elastic and inelastic α-particle scattering using a density-dependent force, *Nucl. Phys. A*, 425: 205-232.

Li Q-R, Yang Y-X. (1993). Alpha-particle elastic scattering on ^{16}O in the four α-particle model. *Nucl Phys. A*, 561: 181-188.

Mahaux C, Ngo H. (1982). Polarization and correlation contributions to the shell-model potential in ^{40}Ca and ^{208}Pb. *Nucl. Phys. A*, 378(2): 205-236.

Mahaux C, Ngo H, Satchler GR. (1986). Causality and the threshold anomaly of the nucleus-nucleus potential. Nucl. Phys. A, 449(2): 354-394.

Michel F, Reidemeister G, Ohkubo S. (1986). Evidence for Alpha-Particle Clustering in the ^{44}Ti Nucleus. *Phys. Rev. Lett.*, 57: 1215-1218.

Michel F, Reidemeister G, Kondō Y. (1995). A potential deduced from low energy ^{16}O(α,α) elastic scattering. *Phys. Rev. C*, 51: 3290-3303.

Nagarajan MA, Mahaux CC, Satchler GR. 1985. Dispersion relation and the low-energy behavior of the heavy-ion optical potential. *Phys. Rev. Lett*., 54(11): 1136.

Neu R, Abele H, Jaentsch H, Striebel C, Staudt G, Walz M, Eversheim PD, Hinterberger F, Oberhummer H. (1989). Folding potential analyses of elastic and inelastic α-scattering processes and of direct (p, α) and (α, p) reactions on light nuclei. *J. Phys. Soc. Jap. Suppl*., 58: 574-580.

Neu R, Welte S, Clement H, Hauser HJ, Staudt G, Müther H. (1989). Coupled-channel analysis of elastic and inelastic alpha scattering on Mg^{24} in the energy range 28-120 MeV. *Phys. Rev. C*, 39(6):2145.

Ornelas A, Kiss GG, Mohr P, Galaviz D, Fülöp Z, Gyürky G, Máté Z, Rauscher T, Somorjai E, Sonnabend K, Zilges A. (2015). The ^{106}Cd(α, α)^{106}Cd elastic scattering in a wide energy range for *g* process studies. *Nucl. Phys. A*, 940: 194-209.

Sack S, Biedenharn LC, Breit G. (1954). The Elastic Scattering of Protons by Alpha Particles. *Phys. Rev*., 93(2): 321.

Singh PP, Schwandt P, Yang GC. (1975). Folding-model analysis of elastic alpha-nucleus scattering. *Phys. Lett. B*, 59(2): 113-117.

Tariq ASB, Rahman AFMM, Das SK, Mondal AS, Uddin MA, Basak AK, Sen Gupta HM, Malik FB. (1999). Potential description of anomalous large angle scattering of α particles. *Phys. Rev. C*, 59: 2558-2566.

Trombik G, Eberhardand KA, Eck JS. (1975). Back-angle anomalies in alpha scattering: Inelastic scattering from the calcium isotopes. *Phys. Rev. C*, 11**:** 685-692.

Yang Y-X, Li Q-R. (1993). A Description of α+^{16}O Elastic Scattering near *E/A*=12 and 7 MeV by a Single-Folding Potential. *Europhys. Lett*., 21: 657-660.